

Jamming Criticality Revealed by Removing Localized Buckling Excitations

Patrick Charbonneau,^{1,2} Eric I. Corwin,³ Giorgio Parisi,⁴ and Francesco Zamponi⁵

¹Department of Chemistry, Duke University, Durham, North Carolina 27708, USA

²Department of Physics, Duke University, Durham, North Carolina 27708, USA

³Department of Physics, University of Oregon, Eugene, Oregon 97403, USA

⁴Dipartimento di Fisica, Sapienza Università di Roma, INFN, Sezione di Roma I, IPFC-CNR, Piazzale Aldo Moro 2, I-00185 Roma, Italy

⁵LPT, École Normale Supérieure, UMR 8549 CNRS, 24 Rue Lhomond 75005, France

(Received 13 November 2014; published 27 March 2015)

Recent theoretical advances offer an exact, first-principles theory of jamming criticality in infinite dimension as well as universal scaling relations between critical exponents in all dimensions. For packings of frictionless spheres near the jamming transition, these advances predict that nontrivial power-law exponents characterize the critical distribution of (i) small interparticle gaps and (ii) weak contact forces, both of which are crucial for mechanical stability. The scaling of the interparticle gaps is known to be constant in all spatial dimensions d —including the physically relevant $d = 2$ and 3 , but the value of the weak force exponent remains the object of debate and confusion. Here, we resolve this ambiguity by numerical simulations. We construct isostatic jammed packings with extremely high accuracy, and introduce a simple criterion to separate the contribution of particles that give rise to localized buckling excitations, i.e., bucklers, from the others. This analysis reveals the remarkable dimensional robustness of mean-field marginality and its associated criticality.

DOI: 10.1103/PhysRevLett.114.125504

PACS numbers: 63.50.Lm, 45.70.-n, 61.20.-p, 64.70.kj

Introduction.—The analogy between glasses and sand-piles, which are both rigid and disordered, was first proposed by Bernal [1], who pioneered comparing their structure. The analogy received renewed attention following the suggestion of Liu and Nagel that different disordered solids could be described by the same jamming phase diagram [2]. Motivated by the ubiquity of jamming in materials physics, an intense research effort from the soft and granular matter community, on the one hand, and from the statistical mechanics of disordered systems community, on the other, has since ensued [3–5].

Recent theoretical breakthroughs have succeeded in transforming this analogy into a solid predictive framework. Quite remarkably, results from what appeared, at first, to be two independent lines of work now point towards a unifying view of the glass problem, understood as encompassing a broad range of amorphous materials. First, the exact infinite-dimensional (mean-field) solution of the celebrated hard-sphere model precisely unifies glass formation and jamming [5–9]. This $d = \infty$ solution predicts, from first principles, that jammed packings are mechanically stable but only marginally so [8,9]. The packings are, therefore, isostatic [[10] Sec. I]; i.e., the number of interparticle contacts matches Maxwell’s criterion for mechanical stability [3,4]. The solution further predicts a (nontrivial) criticality near jamming [8,9]. Second, a real-space description of elementary excitations near jamming finds that soft modes pervade in that regime [11,12]. This approach further provides scaling relations

between the jamming critical exponents, based on marginal stability [13–17].

Both approaches agree that two power-law exponents characterize the structure of disordered jammed packings. The distribution (i) of spatial gaps between particles that are nearly (but not quite) in contact and, hence, of the average number of neighbors away from a sphere surface, scales as $Z(h) - Z(0) \sim h^{1-\gamma}$ for small h , where $h = (r - \sigma)/\sigma$ is the gap size for spheres of diameter σ [18], and (ii) of weak forces f between spheres scales as $P(f) \sim f^{\theta_f}$ for small f . The $d = \infty$ solution further predicts $\gamma = 0.41269\dots$ and $\theta_f = 0.42311\dots$ [8,9].

For isostatic jammed packings, it is found that opening a force contact between particles destabilizes the system by creating a soft mode [[10] Sec. IG], which is a collective particle excitation that preserves the remaining contacts [13,14,16,19]. Phenomenologically, it was noted that some of the resulting excitations are extended, while others are localized [13]. This distinction suggests the existence of two different force exponents: $P(f) \sim f^{\theta_e}$ for contacts associated with extended modes, and $P(f) \sim f^{\theta_\ell}$ for contacts associated with localized modes. The observed total force distribution, which is a weighted average of the two, should, therefore, have the asymptotic form $P(f) \sim f^{\theta_f}$, with $\theta_f = \min(\theta_e, \theta_\ell)$. Marginal mechanical stability analysis provides universal scaling relations for the exponents: $\theta_\ell = 1 - 2\gamma$ and $\theta_e = \theta_\ell/\gamma$ [13–16].

We are now, however, left with a conundrum. Using $\gamma = 0.41269$ from the $d = \infty$ solution with the scaling

relations derived from marginal stability gives $\theta_e = 0.42311$ and $\theta_\ell = 0.17462$. The $d = \infty$ solution, thus, exactly obeys the scaling relations, but only if one assumes $\theta_f = \theta_e$. Yet, this assumption is inconsistent with the relation $\theta_f = \min(\theta_e, \theta_\ell) = \theta_\ell$, which must be true if localized modes exist with finite probability.

The situation is further muddled by the currently available numerical estimates for γ and θ_f in finite d . The value $\gamma = 0.40(2)$ is found to remain unchanged for all $d \geq 2$ [13,16,20–22], and is consistent with the $d = \infty$ solution. The upper critical dimension for the jamming transition may, thus, be as low as $d_u = 2$ [21,22], with all jamming critical exponents being constant for $d \geq 2$. Reported values for θ_f , however, range from 0 [23,24] to 0.42 [22]. Encouragingly, for $d = 2$ the most reliable determinations found $\theta_f = 0.18(2)$ [13,16], independently of the interaction potential [[10] Sec. IH]. For $d = 3$, however, no such agreement is observed and the results even depend on microscopic details of the system [16]. In this Letter, we resolve this perplexing situation by identifying a simple geometrical criterion associated with localized modes, which allows us to accurately study the weak tail of the force distribution.

Isostaticity and the force network.—Consider a packing with $i = 1 \cdots N$ particles located in positions $\mathbf{r}_i = \{r_{i\alpha}\}$ in $\alpha = 1 \cdots d$ dimensions with $\langle ij \rangle = 1 \cdots N_c$ contacts, where $i < j$. At the jamming transition, particles do not overlap, hence, $|\mathbf{r}_j - \mathbf{r}_i| \geq \sigma_{ij}$, where $\sigma_{ij} = (\sigma_i + \sigma_j)/2$ is the sum of particle radii. Two particles are in contact if $|\mathbf{r}_j - \mathbf{r}_i| = \sigma_{ij}$, and in this case, they exchange a radial force along the contact vector $\mathbf{n}_{ij} = (\mathbf{r}_j - \mathbf{r}_i)/|\mathbf{r}_j - \mathbf{r}_i|$. The scalar contact force $f_{ij} = f_{ji}$ on each contact defines $\vec{f} = \{f_{ij}\}$, an N_c -dimensional vector, and the external forces $F_{i\alpha}$ define an Nd -dimensional vector $\vec{F} = \{F_{i\alpha}\}$. The force balance equations for particle i , given the set ∂i of particles in contact with it, then reads

$$F_{i\alpha} = \sum_{j \in \partial i} n_{ji}^\alpha f_{ji} \Rightarrow \vec{F} = \mathcal{S}^T \vec{f}, \quad (1)$$

where \mathcal{S} is a $N_c \times Nd$ matrix with elements $\mathcal{S}_{(ij)}^{\alpha\alpha} = (\delta_{jk} - \delta_{ik})n_{ij}^\alpha$ [[10] Sec. IA]. For a system under cubic periodic boundary conditions and in mechanical equilibrium under no external force, i.e., $\vec{F} = \vec{0}$, Eq. (1) gives Nd homogeneous linear equations for the N_c contact forces, i.e., $\mathcal{S}^T \vec{f} = 0$. The contact vector \vec{f} is, therefore, a zero mode of \mathcal{S}^T . For convenience, we define the $N_c \times N_c$ symmetric matrix $\mathcal{N} = \mathcal{S}\mathcal{S}^T$, which has all the zero modes of \mathcal{S}^T , but may also have additional ones [[10] Sec. IC].

After taking into account global translational invariance, Eq. (1) results in a system of $(N-1)d$ homogeneous linearly independent equations over N_c variables [[10] Sec. IA] and, therefore, admits $\max\{N_c - (N-1)d, 0\}$

nonzero linearly independent solutions. It has been argued further that jamming takes place in the isostatic limit [13,14,21,25], which corresponds to the existence of a single solution to $\mathcal{S}^T \vec{f} = 0$ [Eq. (1)], and hence, $N_c = (N-1)d + 1$ under periodic boundary conditions [[10] Secs. IF and IIA]. Note that, in the thermodynamic limit, the average particle connectivity, $Z(0) = 2N_c/N$, converges to the usual Maxwell criterion for mechanical stability, $\lim_{N \rightarrow \infty} Z(0) = 2d$, consistently with the $d = \infty$ solution [[10] Sec. IIA]. For an isostatic system, \mathcal{N} has a unique zero mode [[10] Sec. IF], and because $\mathcal{N} = \mathcal{S}\mathcal{S}^T$ we also have $\mathcal{N}\vec{f} = 0$. The solution vector \vec{f} must, therefore, be the unique zero mode of \mathcal{N} , with an overall scale factor corresponding to the global pressure. In summary, given the orientation vectors for each pair of contacts in an isostatic packing, the distribution of contact forces can be uniquely determined by finding the eigenvector corresponding to the zero eigenvalue of \mathcal{N} .

Numerical construction of jammed packings and calculation of the forces.—Several protocols have been proposed to construct jammed packings of frictionless spheres, see, e.g., [13,21–26]. Some of them, however, do not systematically result in packings that are precisely isostatic [[10] Sec. IIA]. Because the scaling laws between the jamming exponents follow from isostaticity [14–16], this requirement is strictly enforced here [[10] Sec. IIB]. Isostatic packings under periodic boundary conditions are numerically obtained by minimizing the energy of athermal soft spheres with a quadratic contact potential on general purpose graphical processing units using quad-precision calculations [22,27,28]. Our protocol begins with N_i randomly distributed particles at a packing fraction φ that is roughly twice the final jamming density φ_J . An isostatic point is approached by successively minimizing the system potential energy U using a FIRE algorithm [29], and then shrinking the particle radii. The isostatic configuration can be efficiently approached by exploiting the scaling $U \propto (\varphi - \varphi_J)^2$ [22,23,30] to iteratively estimate the value of φ_J , and then target a new density at an energy that is a fixed fraction of the previous one [[10] Sec. IIB]. For $d = 3$ and 4, we thereby obtained approximately 100 single-component systems with $N_i = 16384$, and 100 equimolar binary mixtures with $N_i = 4096$ in $d = 2$ with a diameter ratio of 1:1.4. A more limited set of configurations was also obtained for $N_i = 4096$ in $d = 5$ –8. In all cases, the choice of system and preparation protocols are known to fully suppress crystallization [20,22,31,32]. Note that applying this same preparation protocol to any other contact potential form (e.g., Hertzian) would also result in configurations that are valid hard sphere packings [[10] Sec. I]. Although the specific packing sensitively depends on the choice of contact potential, algorithm details, and initial configuration, similar structural scaling relations are known to be robustly independent of this choice [13,16,22].

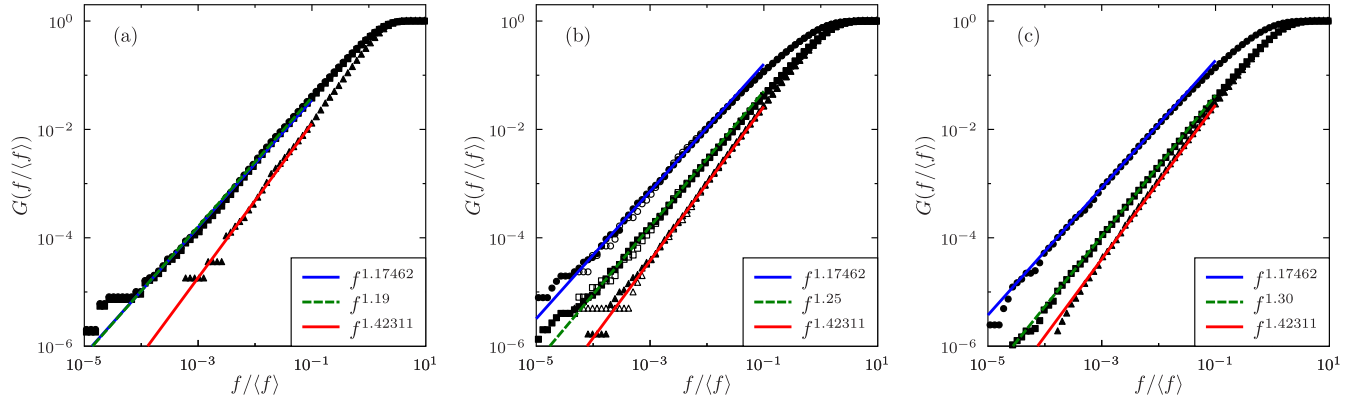


FIG. 1 (color online). Cumulative force distribution $G(f)$ for $d = 2, 3$, and 4 , in (a), (b), and (c), respectively. The distributions $P(f)$ (square), $P_e(f)$ (circle), and $P_e(f)$ (triangle) all show power-law scalings at small forces (in $d = 2$, squares and circles are nearly superimposed because of the large proportion of bucklers), but with different exponents. For the combined distribution, θ_f grows steadily with d , but $P_e(f)$ and $P_e(f)$ are consistent with the exponents obtained by combining the $d = \infty$ solution with marginal stability arguments, i.e., $\theta_e = 0.17462$ and $\theta_e = 0.42311$, respectively. In $d = 2$, the results for θ_e are consistent with those obtained by ranking contacts based on the coupling of their related soft modes to external forces [13]. In $d = 3$, comparing two system sizes, $N_i = 16384$ (full symbols) and $N_i = 1024$ (empty symbols), confirms the absence of significant finite-size effects.

We analyze the contact network at φ_j by first eliminating particles with $Z < d + 1$ contacts, i.e., the rattlers (Fig. 2) [23,24]. After this step, most configurations have $N_c = (N - 1)d + 1$, where N is the number of remaining particles. We discard the configurations for which this condition is not satisfied [[10] Sec. IIC]. In principle, the minimization procedure also outputs the force vector \vec{f} , but extracting small forces from it requires an even heavier use of quad-precision arithmetics than what we have used for the energy minimization [[10] Sec. IIC]. Instead, we determine \vec{f} as the zero mode of \mathcal{N} for this packing [[10] Sec. IF], for which double precision arithmetics suffices. Because \mathcal{N} is sparse, the eigenvector corresponding to the zero mode can efficiently be extracted with the Lanczos algorithm [[10] Sec. IIC], as implemented in MATHEMATICA [33,34].

Results.—Figure 1 gives the cumulative force distribution $G(f) = \int_0^f P(f')df'$ for $d = 2, 3$, and 4 . In all cases, a power-law scaling at weak forces is detected, but the value of θ_f is found to increase with d . Recall that, over the same d range, γ remains robustly constant [22] and is consistent with $\gamma = 0.41269$ from the $d = \infty$ solution [8,9]. The changing value of θ_f with d is, therefore, inconsistent with the scaling relations between exponents θ and γ in a marginally stable phase [13–16].

Soft mode excitations suggest a possible way to resolve this paradox [13,15,16]. The proposed mechanism for localized excitations is for a particle to have all but one of its contact vectors be nearly coplanar [13]. The remaining contact must necessarily be weak (by force balance). Breaking that contact should then result in facile back and forth buckling. Because this motion does not affect the rest of the packing much, the resulting excitation is fairly localized (Fig. 2). Although a nearly coplanar arrangement

of neighbors is formally possible for a particle with any Z , in a sufficiently disordered (noncrystalline) system, it grows increasingly unlikely with Z . This arrangement is, therefore, most likely to occur for particles that have the

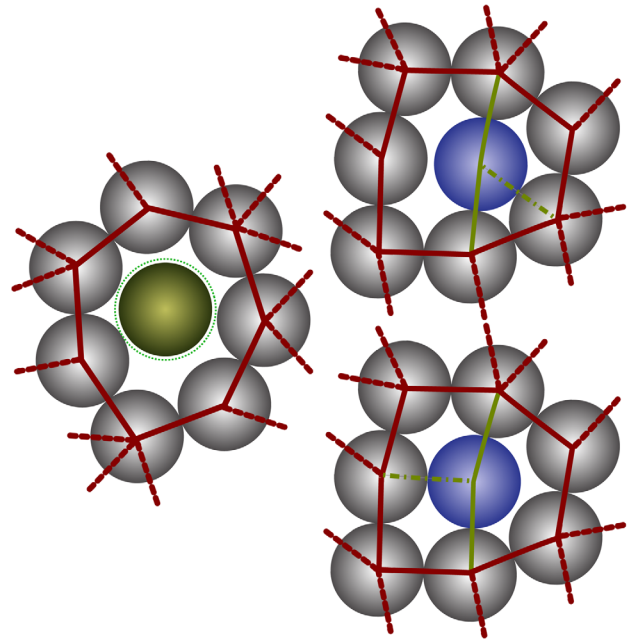


FIG. 2 (color online). Schematic depiction of (left) rattlers and (right) bucklers. At jamming, rattlers (also known as floaters—green) are not part of the force network. Their neighbors (grey) are part of the force network (red lines) and form a rigid cage within which the rattler can freely move (dashed green line). By contrast, bucklers are part of the force network (red and green lines), but breaking their weakest contact (dotted-dashed green line) only creates a localized excitation (top and bottom). Bucklers are, thus, typically particles with d nearly coplanar stronger contacts and a weaker $d + 1$ th contact that balances the resulting normal force.

minimal Z for maintaining local stability, i.e., $Z = d + 1$. Particles with $Z = d + 1$ contacts and for which one contact is weak (we dub them bucklers) are also overwhelmingly likely to have the other d contact particles be nearly coplanar with the center of mass [[10] Sec. IID]. Any other arrangement would entail the presence of at least two weak contacts, which is highly unlikely. In summary, with high probability, all bucklers have $d + 1$ contacts and all particles with $d + 1$ contacts and a weak force are bucklers. In Fig. 1, we consider $P_\ell(f)$ the distribution of all forces involving particles with $d + 1$ contacts (and, thus, all bucklers), and $P_e(f)$ that of the remaining contact forces. This breakdown cleanly separates the power-law regimes for θ_e and θ_ℓ . Remarkably (this is our main result), $P_\ell(f) \sim f^{\theta_\ell}$ while $P_e(f) \sim f^{\theta_e}$, with exponents independent of d and consistent with the $d = \infty$ solution and the scaling relations.

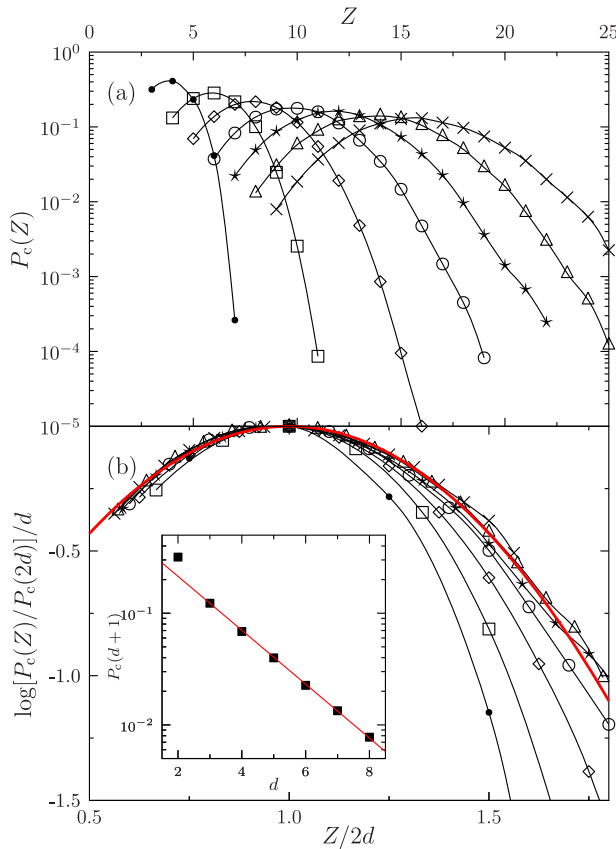


FIG. 3 (color online). (a) Probability distribution of the number of contacts Z for particles within the force network (neglecting rattlers) at jamming in $d = 2, \dots, 8$, from left to right, for the protocol described in the text. Note that the distribution peaks around $Z = 2d$. (b) Rescaling these distributions using a large-deviation form shows the results to converge fairly quickly with d . For this preparation protocol, the form is nearly Gaussian (red line). The large deviation form suggests that the proportion of particles with $Z = d + 1$ (and, thus, of bucklers) decays exponentially with d , (inset) as is explicitly observed in finite d (red line).

This finding also provides an explanation for the behavior of θ_f . In order to see why, let us define the distribution of the number of contacts $P_c(Z)$ [$\sum_Z Z P_c(Z) \approx 2d$]. The fraction of forces adjacent to bucklers is then $n_\ell = (d + 1)P_c(d + 1)/2d$, and the total force distribution

$$P(f) = n_\ell P_\ell(f) + (1 - n_\ell) P_e(f). \quad (2)$$

For large d , it is reasonable to expect that $P_c(Z) \sim e^{d\eta_c(Z/d)}$ becomes strongly peaked (in relative terms) around the average of Z , and is roughly Gaussian around that average. Figure 3 confirms this hypothesis, and as a result, $P_c(d + 1)$ and $n_\ell \sim P_c(d + 1)/2$ both decrease exponentially with d . For small f , it follows that $P(f) \sim n_\ell f^{\theta_\ell} + (1 - n_\ell) f^{\theta_e}$. Hence, it is correct that, asymptotically, one should observe $\theta_f = \min(\theta_e, \theta_\ell)$, but only when $n_\ell f^{\theta_\ell} \gg f^{\theta_e}$, i.e., for forces exponentially small in d . This result explains why no trace of bucklers nor of localized modes can be found in the $d = \infty$ solution, for which $n_\ell = 0$ and, thus, $\theta_f = \theta_e$. It also suggests that the contribution of bucklers cannot be perturbatively detected around that solution either. In the force regime that is numerically (and experimentally) accessible in low d , however, an effective mixed value for θ_f is observed, which is close to θ_ℓ in $d = 2$ and increases smoothly towards θ_e as d increases, reflecting the systematic decrease of n_ℓ .

Conclusion.—Our results demonstrate that the jamming criticality remains robustly constant for $d \geq 2$, although the spurious contribution of rattlers and bucklers must be excluded from the structural analysis in order to cleanly detect it. This remarkable outcome confirms that certain aspects of mean-field marginality subsist in finite-dimensional systems, including in experimentally relevant $d = 2$ and 3 [8,9]. These results should, therefore, be experimentally verifiable.

The theoretical explanation as to why long-wavelength fluctuations do not renormalize the properties of jamming criticality in these systems remains, thus far, unanswered (see [35] for a preliminary investigation). One may argue that the complete absence of thermal fluctuations at jamming, and/or the presence of long-ranged elastic interactions [17], play a role. This observation would then suggest that marginal systems with other types of disorder, be it related to constraint satisfaction or size dispersity, may also exhibit similarly robust mean-field criticality upon approaching their ground state. It is important to note, however, that this universality does not imply that, away from jamming, thermal fluctuations may not destroy the mean-field marginal state structure and round off the associated phase transitions [35].

We acknowledge many fruitful exchanges with L. Berthier, G. Biroli, E. DeGiuli, C. Goodrich, Y. Jin, E. Lerner, A. Liu, P. Urbani, and M. Wyart. We gratefully acknowledge help from C. Barbieri at Sapienza and

M. Peterson at Duke with computational assistance. The European Research Council has provided financial support through ERC Grant Agreement No. 247328. E. I. C. thanks the NSF for support under CAREER Award No. DMR-1255370. P. C. acknowledges support from the National Science Foundation Grant No. NSF DMR-1055586 and the Sloan Foundation. The use of the ACISS supercomputer is supported under a Major Research Instrumentation Grant, Office of Cyber Infrastructure, No. OCI-0960354.

-
- [1] J. D. Bernal, *Nature (London)* **183**, 141 (1959).
 [2] A. J. Liu and S. R. Nagel, *Nature (London)* **396**, 21 (1998).
 [3] M. van Hecke, *J. Phys. Condens. Matter* **22**, 033101 (2010).
 [4] S. Torquato and F. H. Stillinger, *Rev. Mod. Phys.* **82**, 2633 (2010).
 [5] G. Parisi and F. Zamponi, *Rev. Mod. Phys.* **82**, 789 (2010).
 [6] J. Kurchan, G. Parisi, and F. Zamponi, *J. Stat. Mech.* (2012) P10012.
 [7] J. Kurchan, G. Parisi, P. Urbani, and F. Zamponi, *J. Phys. Chem. B* **117**, 12979 (2013).
 [8] P. Charbonneau, J. Kurchan, G. Parisi, P. Urbani, and F. Zamponi, *Nat. Commun.* **5**, 3725 (2014).
 [9] P. Charbonneau, J. Kurchan, G. Parisi, P. Urbani, and F. Zamponi, *J. Stat. Mech.* (2014) P10009.
 [10] See Supplemental Material at <http://link.aps.org/supplemental/10.1103/PhysRevLett.114.125504> for an extended consideration of the excitations in a marginal system, for detailed discussion of isostaticity, and for numerical protocol details.
 [11] M. Wyart, L. E. Silbert, S. Nagel, and T. Witten, *Phys. Rev. E* **72**, 051306 (2005).
 [12] C. Brito and M. Wyart, *J. Chem. Phys.* **131**, 024504 (2009).
 [13] E. Lerner, G. Düring, and M. Wyart, *Soft Matter* **9**, 8252 (2013).
 [14] M. Wyart, *Phys. Rev. Lett.* **109**, 125502 (2012).
 [15] E. DeGiuli, A. Laversanne-Finot, G. A. Düring, E. Lerner, and M. Wyart, *Soft Matter* **10**, 5628 (2014).
 [16] E. DeGiuli, E. Lerner, C. Brito, and M. Wyart, *Proc. Natl. Acad. Sci. U.S.A.* **111**, 17054 (2014).
 [17] M. Müller and M. Wyart, *Annu. Rev. Condens. Matter Phys.* **6**, 177 (2015).
 [18] $Z(h)$ is also the integral of the radial pair distribution function, i.e., $Z(h) = \rho \int_0^{(1+h)\sigma} g(r) dr$, where ρ is the system density. Its critical decay is, therefore, $g(h) \sim h^{-\gamma}$.
 [19] E. DeGiuli, A. Laversanne-Finot, G. Düring, E. Lerner, and M. Wyart, *Soft Matter* **10**, 5628 (2014).
 [20] M. Skoge, A. Donev, F. H. Stillinger, and S. Torquato, *Phys. Rev. E* **74**, 041127 (2006).
 [21] C. P. Goodrich, A. J. Liu, and S. R. Nagel, *Phys. Rev. Lett.* **109**, 095704 (2012).
 [22] P. Charbonneau, E. I. Corwin, G. Parisi, and F. Zamponi, *Phys. Rev. Lett.* **109**, 205501 (2012).
 [23] C. S. O’Hern, S. A. Langer, A. J. Liu, and S. R. Nagel, *Phys. Rev. Lett.* **88**, 075507 (2002).
 [24] A. Donev, S. Torquato, and F. H. Stillinger, *Phys. Rev. E* **71**, 011105 (2005).
 [25] A. B. Hopkins, F. H. Stillinger, and S. Torquato, *Phys. Rev. E* **88**, 022205 (2013).
 [26] S. Torquato and Y. Jiao, *Phys. Rev. E* **82**, 061302 (2010).
 [27] P. K. Morse and E. I. Corwin, *Phys. Rev. Lett.* **112**, 115701 (2014).
 [28] NVIDIA, “Double-double precision arithmetic,” <https://developer.nvidia.com/rdp/assets/double-double-precision-arithmetic> (2013), last accessed November 14, 2014.
 [29] E. Bitzek, P. Koskinen, F. Gähler, M. Moseler, and P. Gumbsch, *Phys. Rev. Lett.* **97**, 170201 (2006).
 [30] H. Jacquin, L. Berthier, and F. Zamponi, *Phys. Rev. Lett.* **106**, 135702 (2011).
 [31] D. N. Perera and P. Harrowell, *Phys. Rev. Lett.* **81**, 120 (1998).
 [32] J. A. van Meel, B. Charbonneau, A. Fortini, and P. Charbonneau, *Phys. Rev. E* **80**, 061110 (2009).
 [33] C. Lanczos, *J. Res. Natl. Bur. Stand.* **45**, 255 (1950).
 [34] MATHEMATICA, Version 10.0 Wolfram Research, Inc., 2014.
 [35] P. Urbani and G. Biroli, arXiv:1410.4523.